JOURNAL OF MATERIALS SCIENCE 19 (1984) 1131–1144

Influence of impurities on the etching of NaCl crystals

K. SANGWAL, G. ZANIEWSKA
Institute of Physics, Technical University of Łódź, Wólczańska 219, 93 005 Łódź, Poland

The effect of $CdCl_2$, $CuCl_2 \cdot 2H_2O$, $MnCl_2 \cdot 4H_2O$ and $FeCl_3 \cdot 6H_2O$ impurities and undersaturation on the rates of macroscopic dissolution, v_p, lateral etching away from a dislocation line, v_t, and normal etching along the dislocation line, v_n, and on the surface micromorphology of the {100} face of NaCl single crystals in water, methanol and 96% ethanol is investigated. The dependence of etch rates on impurity concentration, c_i, showed that the addition of a salt to the solvent always leads to a decrease in v_p, which attains a minimum value after a particular value of c_i. The concentration dependence of v_t and v_n is relatively complex, but often both decrease or increase simultaneously. A change in etch-pit morphology is caused by increasing the concentrations of all additives in ethanol and methanol. The dependence of etch rates on the undersaturation of methanol and methanol containing 10^{-3} M $CdCl_2$ showed that dislocation etch pits are formed only for undersaturations greater than 0.02 and 0.06, respectively. These results as well as the roughening of etched surfaces at low impurity concentrations, the formation of terraced etch pits and the difference between etch pits at aged and fresh dislocations are discussed.

1. Introduction

During the study of the etching behaviour of alkali halide crystals by various solutions, it has been recognized that factors such as nature of solvent, nature and concentration of impurity, temperature, stirring, undersaturation, crystallographic orientation of the surface being etched, segregation of impurities at dislocations and kind of dislocations affect the formation of dislocation etch pits. Only those impurities which are able to slow down the motion of dissolution steps emanating from the dislocations sites produce contrasting etch pits [1–12]. A change in the concentration of inhibiting impurities leads to a change in the morphology of dislocation etch pits [1, 3–5, 7–10, 12]. In some solvents, with an increase in the additive concentration, ⟨100⟩, ⟨110⟩ and finally again ⟨100⟩ pits are obtained [1, 8, 12]. It was also found that at low concentrations of the additive the etched surface is rough, and progressively becomes smoother with an increase in the additive concentration [7, 8, 10, 12]. In some etching solutions, the dislocation etch pits are terraced [1, 13]. Etch rates have also been observed to depend on the nature of a solvent [7, 12, 14], concentration of impurities which are effective in revealing dislocation etch pits [1, 4, 5, 12, 15], stirring [1, 3–5, 15], and temperature of etching [2, 5, 14, 15–17]. With the exception of $FeCl_3$ added to CH_3COOH [15], the macroscopic or gross dissolution rate, v_p, decreases with the addition of the impurity to the solvent [1, 4, 5, 15]. With increasing impurity concentration, the rate of lateral etching away from a dislocation line, v_t, and the rate of normal etching along the dislocation line, v_n, either regularly decrease or increase like v_p [1, 15] or first increase and then decrease exhibiting a maximum [12]. However, despite several studies no clear picture has emerged about the following points.

1. The requirements that an inhibiting impurity should satisfy in order to reveal dislocation etch pits.

2. The sites at which an impurity adsorbs.

0022–2461/84 $03.00 + .12 © *1984 Chapman and Hall Ltd.*

3. The agreement or disagreement between the experimental results and the theory of dislocation etch-pit formation.

4. Surface roughening at low impurity concentration.

5. Terracing of dislocation etch pits.

The investigations carried out so far on alkali halides either deal with the effect of impurities on the formation and morphology of dislocation etch pits or with their effect on etching kinetics. However, for meaningful information on the fundamental processes involved in the formation of dislocation etch pits, it is desirable to investigate dissolution kinetics and micromorphology of etched surfaces simultaneously. In the present paper some results obtained on the effect of impurity concentration and solution undersaturation on dissolution kinetics and surface micromorphology of the {100} surfaces of NaCl crystals are presented and discussed.

In the present work on NaCl, water, methanol and 96% ethanol were used as solvents, while $CdCl_2$, $CuCl_2 \cdot 2H_2O$, $FeCl_3 \cdot 6H_2O$ and $MnCl_2 \cdot 4H_2O$ were selected as the additive. The solvents are essentially the same as have been employed for studying the etching kinetics [4, 5, 14, 18, 19] and the formation and morphology of dislocation etch pits [5, 7–10, 14]. The choice of the additive was guided by the following factors.

1. The addition of these impurities to ethanol and methanol leads to the revelation of etch pits at the sites of dislocations emerging on the {100} faces of NaCl crystals [5, 7–10].

2. Mn^{2+} and Cd^{2+} salts are known to be effective impurities in changing the habit of NaCl crystals growing from aqueous solutions [20, 21].

3. The constitution of complexes formed in solution as a function of salt concentration is known in the case of $CuCl_2 \cdot 2H_2O$ and $FeCl_3 \cdot 6H_2O$ [22–25].

2. Experimental procedure

The samples in the form of rectangular parallelepipeds, having dimensions ranging between 15 mm × 4 mm × 4 mm and 10 mm × 4 mm × 3 mm were prepared by cleavage from a large undoped NaCl crystal grown from the melt following the technique of Voszka *et al.* [26] and were kindly supplied by Dr M. Suszyńska. These specimens were used for etching without any heat treatment, which ensured the presence of some fresh dislocations inctroduced during their preparation and handling. Grain boundaries were present in every sample without exception. The density of dislocation etch pits, excluding those in the sub-boundaries, estimated by using $C_2H_5OH + CdCl_2$ etchant ranged between 10^6 and 10^7 pits cm^{-2}.

The effectiveness of an etching solution was judged from the formation of etch pits at grain boundaries and in the interiors of grains. Since the grain boundaries are formed during growth, they were assumed to be composed of aged disloctions. If an etchant produced etch figures mainly at grain boundaries, it was inferred that they corresponded to the sites of aged dislocations. On the other hand, if an etchant formed pits at grain boundaries and in the interiors of grains such that their total density was of the order of the anticipated one, it was deduced that the pits represented the sites of both aged and fresh dislocations. The experimental method employed for the observation of surface micromorphology and for the determination of etch rates was the same as used previously in the case of MgO crystals [27, 28] with the difference that the etched samples were not rinsed in any solvent. No stirring was employed. For a faster etchant such as CH_3OH and H_2O, v_p and v_t were reproducible within ± 6% and 4%, respectively. For slow etchants (e.g. C_2H_5OH) the reproducibility was, however, somewhat poorer. For larger pits, with a depth of about 7 μm, v_n was reproducible within ± 6%, but for smaller or shallower pits the variation was up to ± 15%. 90% ethanol was used as the polishing solution. For all the etch pit patterns presented in the paper the ⟨100⟩ directions are parallel to the edges of the photographs.

The undersaturated solutions were prepared from a stock saturated solution for a particular solvent. The undersaturation, σ, of a solution was estimated from the relation: $\sigma = (1 - c/c_0)$ where c_0 and c are the equilibrium and actual concentrations of NaCl in a solvent. The driving force for dissolution, $\Delta\mu/kT$, and c/c_0 are related by [21]

$$\Delta\mu/kT = \ln(c/c_0). \qquad (1)$$

3. Experimental results

3.1. Effect of additive concentration on etch pit morphology

3.1.1. $CdCl_2$

Hari Babu and Bansigir [7–10] have studied the dependence of the morphology of etch pits produced on the {100} surfaces of NaCl crystals on the concentration of $CdCl_2$ impurity added to ethanol and methanol. These authors found that at

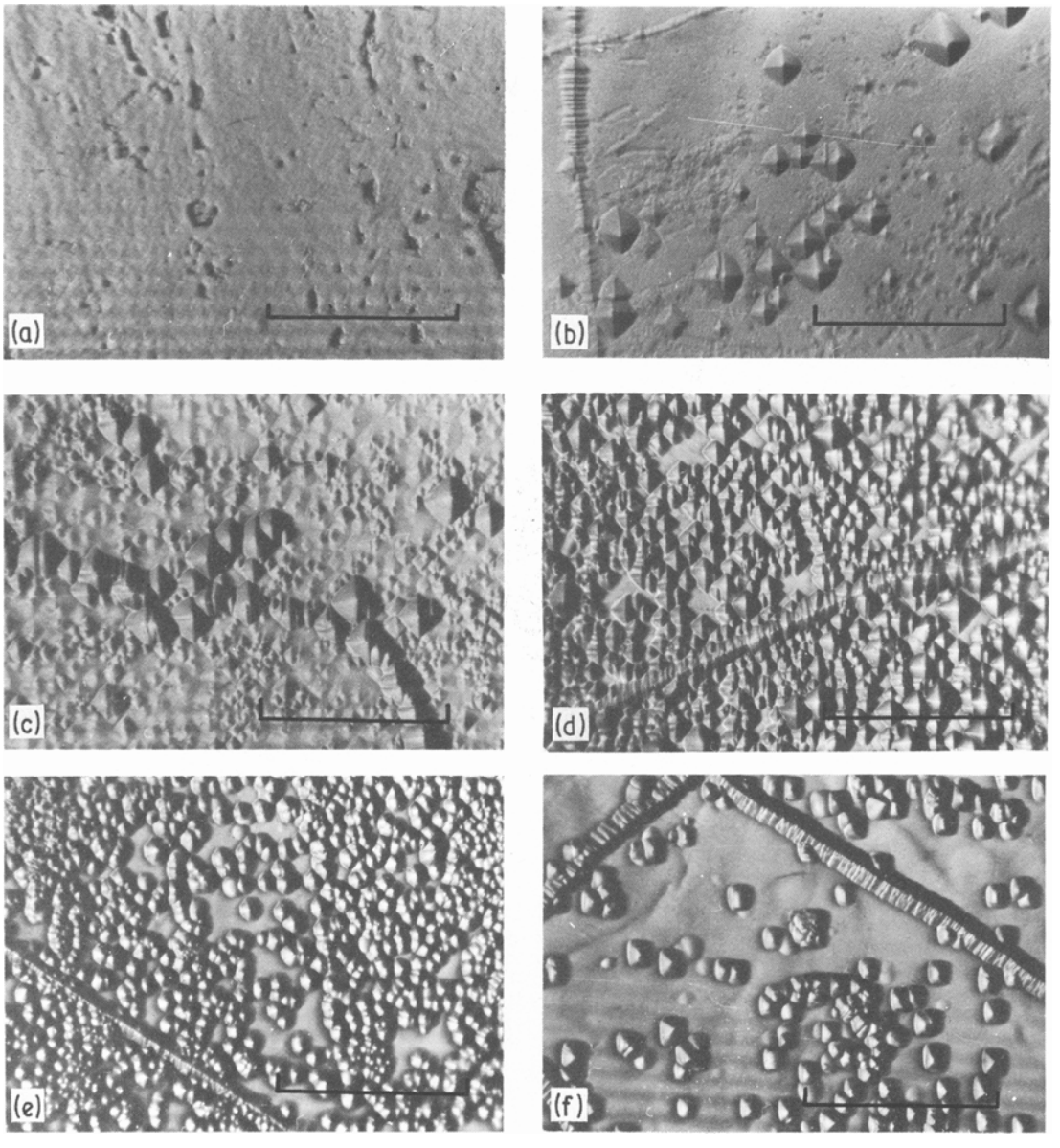

Figure 1 Etch-pit patterns produced by C_2H_5OH containing (a) 10^{-7} M, (b) 10^{-6} M, (c) 10^{-5} M, (d) 10^{-4} M, (e) 10^{-3} M, and (f) 10^{-2} M $CdCl_2$ after 20 min at 25° C. Scale bar = 0.1 mm.

low concentrations of the additive the etched surfaces were mottled and that the size and morphology of etch pits was essentially the same at all additive concentrations. In methanol $CdCl_2$ produced etch pits with beaks and channels at aged dislocations. The inner portions of the etch pits at aged dislocations which did not exhibit beaks were more contrasting. Our results with $CdCl_2 + C_2H_5OH$ are somewhat different in that neither the morphology nor the size of etch pits was the same at low additive concentration. Therefore some photographs are intended to illustrate the difference in the etching characteristics observed in this study.

Pure 96% C_2H_5OH produces ⟨100⟩ orientation pits often with a density of the order of $10^2 cm^{-2}$. These etch pits locate the emergence points of aged dislocations. At a concentration of 10^{-6} M, large dark ⟨110⟩, and additional tiny ⟨100⟩ and rounded etch pits at aged and fresh dislocations are produced, respectively. With a further increase in the additive concentration, ⟨110⟩, ocatagonal

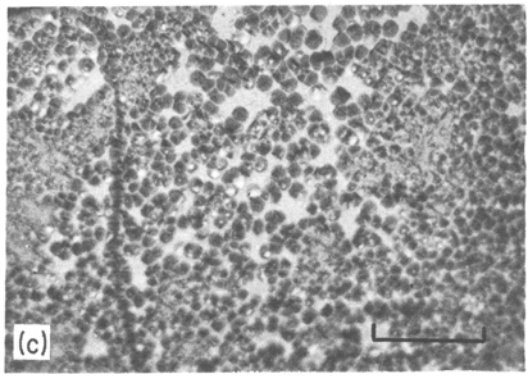

Figure 2 Etch pits produced by CH_3OH containing (a) 1.7×10^{-3} M, (b) 5×10^{-3} M and (c) 5×10^{-2} M $CdCl_2$ after 6 min at 25° C. Scale bar = 0.1 mm.

and ⟨100⟩ pits at both aged and fresh dislocations are formed. The difference in the size of etch pits also decreases with an increase in the salt concentration. These features are illustrated in Fig. 1.

CH_3OH produces ⟨100⟩ pits at the sites of dislocations, as have also been observed by Baranova and Nadgornyi [14]. With an increase in the salt concentration, octagonal, ⟨110⟩ and again octagonal pits at dislocation sites are produced. The inner portions of some of the octagonal and ⟨110⟩ pits formed at low impurity concentrations are more contrasting, but all the pits have essentially the same size. The octagonal etch pits produced at relatively higher impurity concentrations have the same contrast and size. These features of etch pits, illustrated in Fig. 2, show that CH_3OH containing different $CdCl_2$ concentration produces pits at both fresh and aged dislocations. These results are similar to those reported by Hari Babu and Bansigir [10].

A 5% undersaturated solution of H_2O essentially acts as a polishing solution at $CdCl_2$ concentrations below 10^{-5} M. However at about 10^{-5} M, ⟨100⟩ pyramidal hillocks of nondislocation origin are formed. The density of these hillocks changes from one region to another of the etched surface. For $CdCl_2$ concentration above 10^{-4} M, only ⟨100⟩ dislocation etch pits are produced, and these become somewhat rounded at 10^{-1} M. Also, as in the case of CH_3OH, the pits on a surface are almost of the same size, but do not distinguish between aged and fresh dislocations. Examples of these features are shown in Fig. 3.

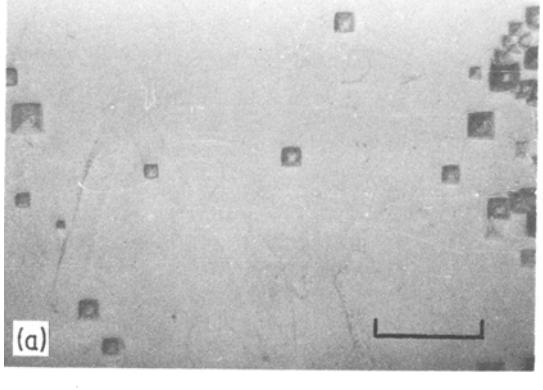

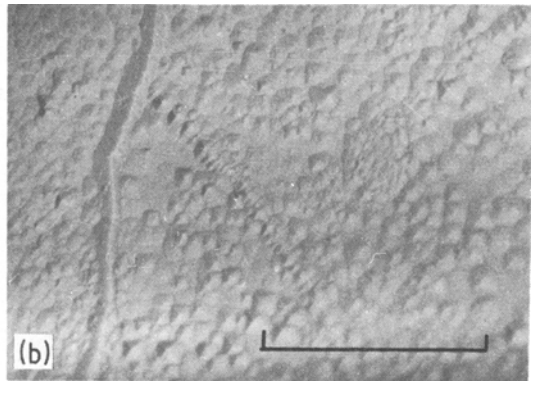

Figure 3 (a) Etch hillocks, and (b) etch pits produced by undersaturated H_2O containing 10^{-5} and 10^{-2} M $CdCl_2$, respectively, after 5 min at 25° C. Scale bar = 0.1 mm.

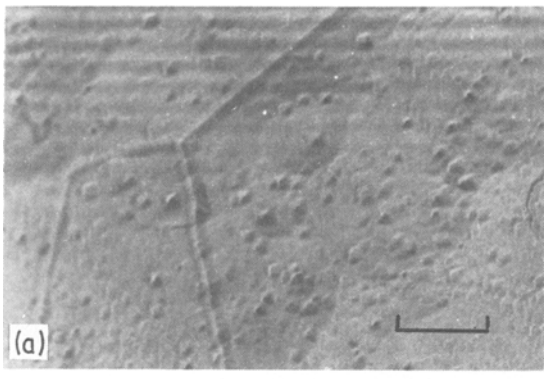

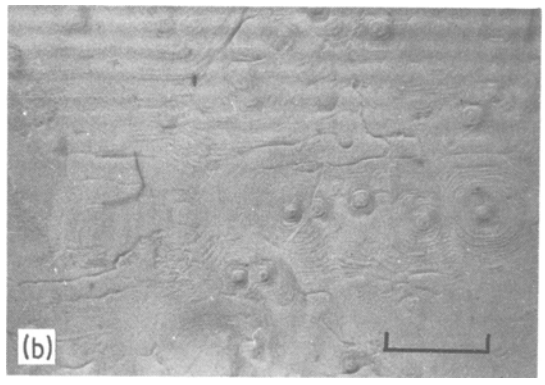

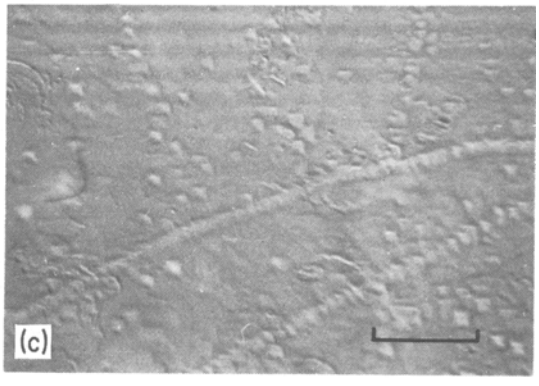

Figure 4 Etch-pit patterns formed by CH_3OH containing different concentrations of $FeCl_3 \cdot 6H_2O$: (a) no impurity, (b) 10^{-4} M, and (c) 10^{-2} M. Etching time for (a) 4 min, and for (b) and (c) 2 min. Scale bar = 0.1 mm.

3.1.2. $FeCl_3 \cdot 6H_2O$

In C_2H_5OH, $FeCl_3 \cdot 6H_2O$ at concentrations greater than 10^{-5} M reveals ⟨100⟩ etch pits corresponding mainly to aged dislocations. In CH_3OH, it yields octagonal etch pits at 10^{-4} and again ⟨100⟩ pits between 10^{-3} and 10^{-2} M (Fig. 4). Above 10^{-1} M the surface becomes rough and etch-pit formation is suppressed.

3.1.3. $CuCl_2 \cdot 2H_2O$

In C_2H_5OH, at low concentrations ⟨100⟩ pits are produced, which change their orientation to ⟨110⟩ with an increase in the salt concentration (Fig. 5). The pits at aged dislocations are larger than those at fresh ones. At higher salt concentrations the surface becomes rough and the etch pits are poorly revealed.

In CH_3OH, with an increase in the salt concentration, ⟨100⟩, octagonal and ⟨110⟩ pits are formed at dislocation sites (Fig. 6). The ⟨100⟩ and octagonal pits are terraced and some of them appear to have even spiral steps. An example of a pit having spiral steps is indicated in Fig. 6b.

3.1.4. $MnCl_2 \cdot 4H_2O$

In C_2H_5OH, $MnCl_2 \cdot 4H_2O$ yields ⟨100⟩ pits at a concentration of 10^{-4} M. The pits become circular above 10^{-3} M. With an increase in the salt concentration, CH_3OH produces ⟨100⟩, circular and ⟨110⟩ pits. The pits formed at aged dislocations are deeper than those at fresh dislocations.

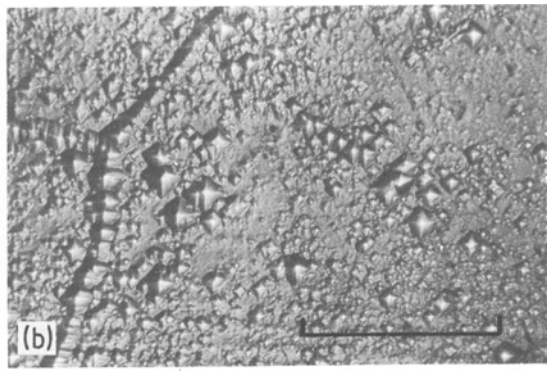

Figure 5 Etch pits revealed by C_2H_5OH containing (a) 10^{-4} M, and (b) 10^{-3} M $CuCl_2 \cdot 2H_2O$ after etching for 20 min at 25° C. Scale bar = 0.1 mm.

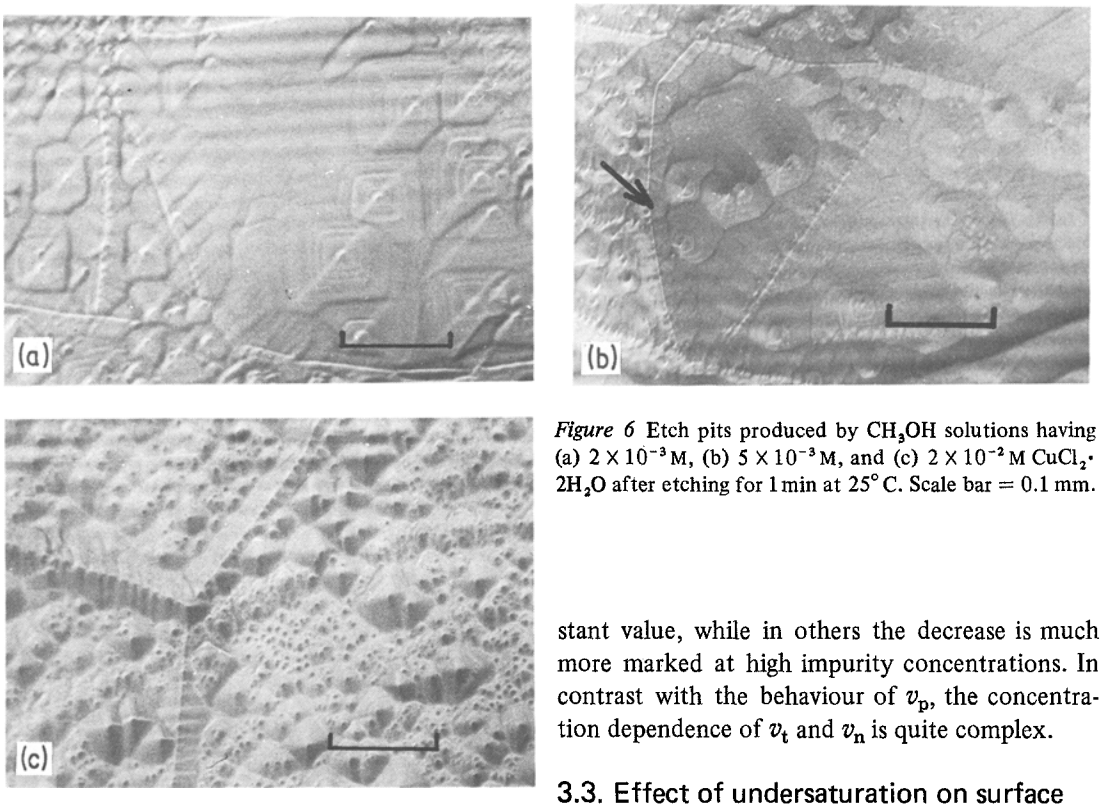

Figure 6 Etch pits produced by CH_3OH solutions having (a) 2×10^{-3} M, (b) 5×10^{-3} M, and (c) 2×10^{-2} M $CuCl_2 \cdot 2H_2O$ after etching for 1 min at 25° C. Scale bar = 0.1 mm.

3.2. Effect of additive concentration on etch rates

The effect of the concentration of the above additive in C_2H_5OH, CH_3OH and 5% H_2O solutions on v_p, v_t and v_n is illustrated in Figs. 7, 8 and 9, respectively. From these figures it may be noted that the addition of a salt to a solvent always leads to a decrease in v_p. In some cases after a particular value of impurity concentration v_p attains a constant value, while in others the decrease is much more marked at high impurity concentrations. In contrast with the behaviour of v_p, the concentration dependence of v_t and v_n is quite complex.

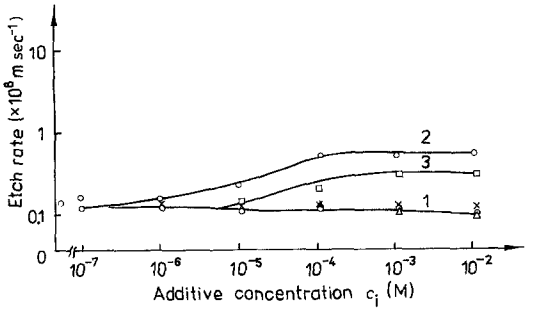

Figure 7 Dependence of v_p, v_t and v_n on the concentrations of different impurities in C_2H_5OH at 25° C. Curve 1 represents v_p for (△) $CuCl_2 \cdot 2H_2O$, (×) $MnCl_2 \cdot 4H_2O$, and (○) for $CdCl_2$; and curves 2 and 3 represent, respectively, v_t and v_n for $CdCl_2$.

3.3. Effect of undersaturation on surface micromorphology and etch rates

The dependence of undersaturation on surface micromorphology and dissolution rates was investigated in H_2O and CH_3OH. In case of H_2O, the surface remains smooth and visible etch pits are not formed at any undersaturation. In CH_3OH which produces dislocation etch pits (see [14] and Section 3.1.1), below about 2% undersaturation dislocations are not active centres for dissolution and surface dissolution is dominant (Fig. 10). In the presence of 10^{-3} M $CdCl_2$, CH_3OH produces dislocation etch pits above about 6% undersaturation. Here with a decrease in undersaturation, the morphology of dislocation etch pits changes from ⟨1 1 0⟩ to circular.

The dependence of etch rates on the undersaturation of H_2O, CH_3OH and $CH_3OH + 10^{-3}$ M $CdCl_2$ is shown in Fig. 11. In H_2O, for which the dependence of v_p on σ was studied up to $\sigma = 0.27$, v_p rapidly increases linearly following the relation $v_p\,(\mathrm{m\,sec^{-1}}) = 1.2 \times 10^{-10}\,\sigma$, while in CH_3OH and $CH_3OH + CdCl_2$, v_p, v_t and v_n appear to increase exponentially with undersaturation. Further, at any value of undersaturation, none of the curves of etch rates in the presence of the additive has a tendency to join the corresponding curves for pure CH_3OH.

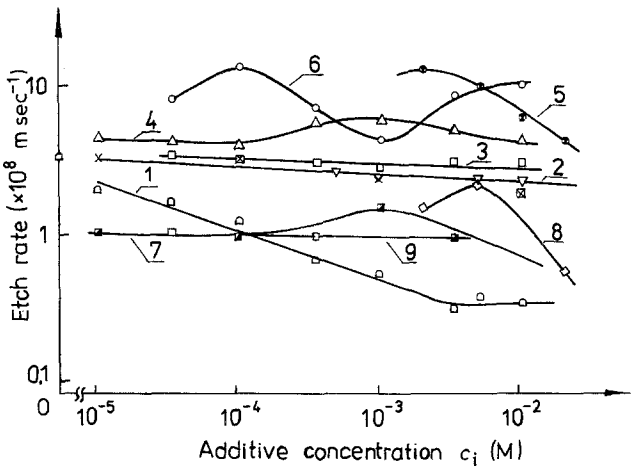

Figure 8 Dependence of v_p, v_n and v_t on the concentration of additives in CH_3OH at 25° C. Curves 1, 2 and 3 are for v_p; curves 4, 5 and 6 for v_t; and curves 7, 8 and 9 for v_n. Curves 1, 4 and 7 are for $CdCl_2$; curves 2, 5 and 8 for $CuCl_2 \cdot 2H_2O$; curve 2 with crosses for $MnCl_2 \cdot 4H_2O$; and curves 3, 6 and 9 for $FeCl_3 \cdot 6H_2O$.

4. Discussion

4.1. Mechanism of adsorption of impurities

4.1.1. v_p *against* c_i *curves*

To analyse the nature of v_p against c_i curves, we consider the following possible relationships:

$$v_p/v_p^0 = Ac_i^n, \quad \text{empirical relation;} \tag{2}$$

$$v_p^0 - v_p = Kc_i^m, \quad \text{Freundlich isotherm;} \tag{3}$$

$$v_p^0 - v_p = K_1c_i/(1 + K_2c_i), \quad \text{Langmuir isotherm;} \tag{4}$$

$$v_p^0 - v_p = B\log C_0 + B\log c_i; \quad \text{Temkin isotherm.} \tag{5}$$

In these equations v_p^0 is the dissolution rate in pure solvent, v_p the dissolution rate in the presence of an impurity, m, n, K, K_1, K_2, A and B are constants, and the reduction in the dissolution rate due to the impurity adsorption on the surface is given here by

$$(v_p^0 - v_p)/v_p^0 = \theta, \tag{6}$$

where θ is the relative surface coverage by the impurity. Constants K_1 and K_2 are given by [29]

$$K_2 = \frac{K_1}{v_p^0} = \exp(-\Delta G_a/RT) \tag{7}$$

while the constant C_0 is expressed by [30, 31]

$$C_0 = \exp(\Delta G_a^0/RT) \tag{8}$$

with

$$\Delta G_a = \Delta G_a^0(1 - b\theta). \tag{9}$$

Here ΔG_a is the differential molar heat of adsorption, ΔG_a^0 the initial heat of absorption when $\theta \to 0$, and b and a are constants.

From Figs. 7, 8 and 9 it appears that, up to the concentrations beyond which after an initial decrease v_p becomes constant, all the curves of v_p against c_i are described by Equation 2 with constants n and A given inTable I. The data for the decreasing value of v_p with increasing c_i were subsequently plotted according to Equations 3, 4 and 5 of the isotherms. It was found that Equation

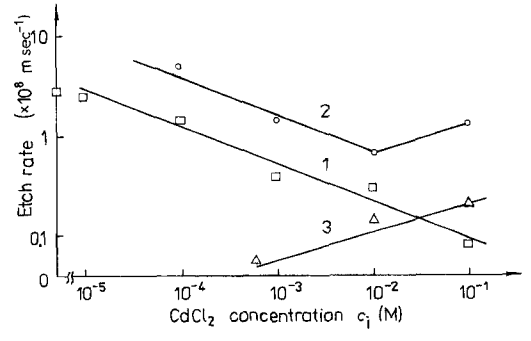

Figure 9 Graph illustrating the dependence of (1) v_p, (2) v_t and (3) v_n on $CdCl_2$ concentration in 5% undersaturated H_2O solution.

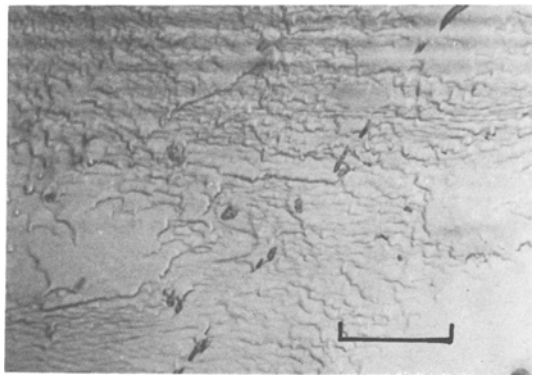

Figure 10 Etch pattern produced by 1% undersaturated CH_3OH solution after etching for 30 min at 25° C. Scale bar = 0.1 mm.

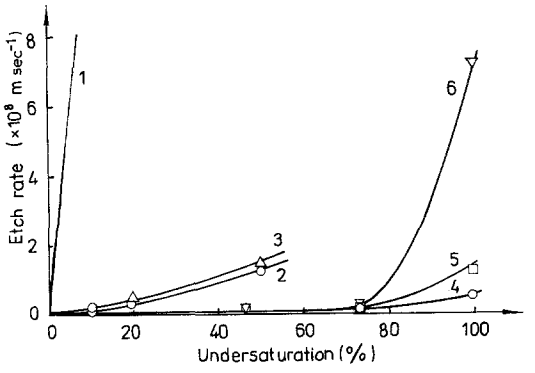

Figure 11 Dependence of v_p (curves 1, 2 and 4) v_t (curves 3 and 6) and v_n (curve 5) for (1) H_2O, (2, 3) CH_3OH and (4, 5, 6) $CH_3OH + 10^{-3}$ M $CdCl_2$ at 25° C.

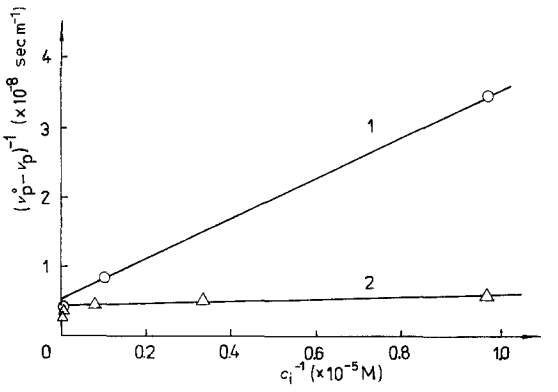

Figure 12 Graph showing the dependence of $(v_p^0 - v_p)^{-1}$ on c_i^{-1} for (1) 5% H_2O, and (2) CH_3OH containing $CdCl_2$ impurity.

3 is not obeyed by any of the impurities in any solvent employed in this study. For example, for 5% undersaturated solution of H_2O containing $CdCl_2$, the value of the constant m decreases from 0.65 at 10^{-5} M to 0.02 at additive concentrations above 10^{-2} M.

Equation 4 is followed by 5% undersaturated $H_2O + CdCl_2$ and $CH_3OH + CdCl_2$ (Fig. 12). In the former case, up to concentrations at which v_p attains a constant value or decreases markedly subsequently, the relationship is followed in the whole concentration interval, but in the latter case the fit is poorer at lower concentrations. For these systems the constants K_1 and K_2 of Equation 4, and the estimated differential heat of adsorption, ΔG_a, obtained by using Equation 6 are listed in Table II.

Equation 5 gives the best fit for the experimental data obtained in CH_3OH (Fig. 13) and C_2H_5OH (Fig. 14). The constants B and $B \log C_0$ of this equation and the values of the heat of absorption, ΔG_a^0, estimated by using Equation 7, are given in Table III.

From Tables II and III it follows that in different solvents the heat of absorption of an impurity increases in the order: H_2O, CH_2OH and C_2H_5OH. Further, in a particular solvent the heat of absorption increases in the sequence: $CdCl_2$, $CuCl_2 \cdot 2H_2O$ equal to $MnCl_2 \cdot 4H_2O$, and $FeCl_3 \cdot 6H_2O$. The ability of solvation of a cation in different solvents decreases in the above order, while the ability of solvation of different cations in a particular solvent increases in the observed order. Thus it may be concluded that the heat of absorption is associated with the ability of solvation of a cation in a particular solvent.

From Table II and III it may be noted that for $CdCl_2$ in CH_3OH and H_2O, $\Delta G_a > \Delta G_a^0$. Since in the Temkin isotherm the heat of absorption is a function of surface coverage, the fact that $\Delta G_a > \Delta G_a^0$ implies that, in the concentration interval where these isotherms hold, the heat of adsorption is somewhat icreased with surface coverage.

The maximum concentration of an additive that effectively reduces v_p in a solvent to a constant level is usually less than 10^{-1} M. Assuming that a molecule of the additive completely dissociates into ions and that an ion moves in the etching medium as in an ideal gas, we may estimate the upper limit of the number, n_i, of ions striking per m^2 per sec by using the relation

$$n_i = z c_i N_A \left(\frac{3KT}{m_a}\right)^{1/2}. \qquad (10)$$

TABLE I Values of constants n and A in the empirical Equation 1

Solvent	Impurity	n	Av_p^0(m sec^{-1})
H_2O	$CdCl_2$	0.40	3.0×10^{-10}
CH_3OH	$CdCl_2$	0.31	5.0×10^{-10}
	$CuCl_2 \cdot 2H_2O$, $MnCl_2 \cdot 4H_2O$	0.032	2.0×10^{-8}
	$FeCl_3 \cdot 6H_2O$	0.005	2.8×10^{-8}
C_2H_5OH	$CdCl_2$	0.008	8×10^{-10}
	$CuCl_2 \cdot 2H_2O$, $MnCl_2 \cdot 4H_2O$	0.006	1×10^{-9}

TABLE II Values of constants K_1 and K_2 in Equation 3, and ΔG_a^0 for $CdCl_2$ impurity

Solvent	K_1(m sec^{-1} M^{-1})	K_2(M^{-1})	ΔG_a^0(kcal mol^{-1})
H_2O	3.20×10^{-4}	1.3×10^4	5.6
CH_3OH	6.67×10^{-3}	2.7×10^5	12.5

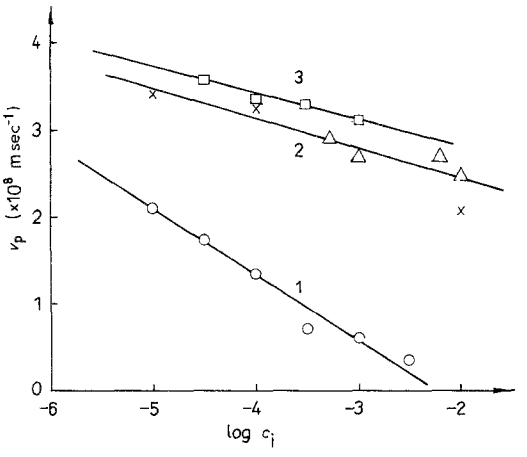

Figure 13 Graph illustrating the dependence of v_p on $\log c_i$ for (1) $CdCl_2$, (2) $CuCl_2 \cdot 2H_2O$ and $MnCl_2 \cdot 4H_2O$, and (3) $FeCl_3 \cdot 6H_2O$ in CH_3OH. The triangles and crosses of curve 2 are for $CuCl_2 \cdot 2H_2O$ and $MnCl_2 \cdot 4H_2O$, respectively.

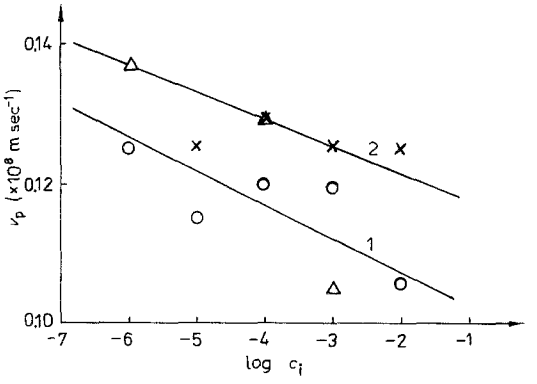

Figure 14 Graph showing the dependence of v_p on $\log c_i$ for (1) $CdCl_2$, and (2) $CuCl_2 \cdot 2H_2O$ and $MnCl_2 \cdot 4H_2O$ in C_2H_5OH. The triangles and crosses of curve 2 are for $CuCl_2 \cdot 2H_2O$ and $MnCl_2 \cdot 4H_2O$, respectively.

Here z is the total number of dissociated ions per molecule of the additive, N_A the Avogadro number equal to 6×10^{23} and m_a the mass of a solvated ion. For $m_a = 200$ a.m.u. $= 200 \times 1.67 \times 10^{-24}$ g, $c_i = 10^{-1}$ M, $z = 3$ and $T = 300$ K, one obtains $n_i \approx 10^{17}$. The number of anions or cations per m^2 of the surface is 10^{19}. Thus we may conclude that at the maximum about 1% of the surface ions are covered by the inhibiting species. Obviously, such a low surface coverage by the absorbate may be taken to be limited to the monomolecular surface layer. This is the reason why Langmuir and Temkin isotherms describe the present data satisfactorily. The values of the heat of absorption indicate that absorption is chemical in nature.

According to Chernov [32, 33], the effect of adsorption of impurities on the growth of F faces can be understood in terms of their absorption time, τ, given by

$$\tau \approx \nu^{-1} \exp(\Delta G_a / kT) \qquad (11)$$

where ν is the frequency factor of the order of $10^{13}\,sec^{-1}$. For chemically adsorbed impurities $\tau \gg \lambda/v$, where λ is the interstep distance and v the rate of motion of steps. In the present case of dissolution of NaCl, for $\lambda = 2.81 \times 10^{-10}$ m and $v_p = 3.7 \times 10^{-8}\,m\,sec^{-1}$, $\lambda/v = 7.5 \times 10^{-3}$ sec for methanol. For the lowest value of $\Delta G_a \approx 6\,kcal\,mol^{-1}$, from Equation 11 one obtains $\tau \approx 10^{-2}$ sec at room temperature. For higher values of ΔG_a, τ will be still larger. Thus we may conclude that the inhibiting species remain immobile during the dissolution of the {100} surfaces of NaCl.

The standard electrode potentials of sodium, manganese, cadmium, iron and copper are −2.714, −1.05, −0.402, −0.036 and 0.345 eV, respectively [34]. If exchange reaction were taking place between the cations of the crystal and the impurity, the effectiveness of the impurity cation in reducing v_p should increase in the above sequence. This is contrary to the experimental results. Thus it may be concluded that exchange reactions of the type encountered in the dissolution of MgO in aqueous solutions of acidic salts [28] do not take place in the macroscopic dissolution of NaCl crystals.

TABLE III Values of constants B and $B \log C_0$ in Equation 4 and $\log C_0$ and ΔG_a^0

Solvent	Impurity	$-B$ (m sec^{-1})	$B \log C_0$ (m sec^{-1})	$-\log C_0$	ΔG_a^0 (kcal mol^{-1})
CH_3OH	$CdCl_2$	7.72×10^{-9}	4.44×10^{-8}	5.75	7.9
	$CuCl_2 \cdot 2H_2O$, $MnCl_2 \cdot 4H_2O$	3.36×10^{-9}	4.44×10^{-8}	13.21	18.2
	$FeCl_3 \cdot 6H_2O$	2.64×10^{-9}	4.44×10^{-8}	16.82	23.2
C_2H_5OH	$CdCl_2$	4.8×10^{-11}	1.36×10^{-9}	28.3	39.0
	$CuCl_2 \cdot 2H_2O$, $MnCl_2 \cdot 4H_2O$	3.7×10^{-11}	1.42×10^{-9}	38.4	53.0

4.1.2. v_t and v_n against c_i curves

In H_2O, with an increase in $CdCl_2$ concentration v_t decreases like v_p up to 10^{-2} M. The slope of the v_t against c_i curves up to 10^{-2} M (exponent n in Equation 2) suggests that in this case surface adsorption is responsible for a decrease in v_t and that the value of ΔG_a is equal to that for macroscopic dissolution. On the other hand, v_n regularly increases from the very beginning with increasing c_i. This is a consequence of an increasing rate of pit nucleation along the dislocation line with increasing c_i. Since the dissolution of NaCl in H_2O is essentially volume-diffusion controlled [18, 35], it may be argued that the addition of an impurity to H_2O modifies the diffusion field around the site of a dislocation such that c/c_0 is increased. This inference is in agreement with the predictions of the theoretical equations of v_n and the free energy change, ΔG_n, involved in the formation of dislocation etch pit of unit depth [36], and also with the conclusions of Ives and Hirth [2] on the dislocation etch-pit formation on the {100} face of LiF.

Above 10^{-2} M $CdCl_2$ in H_2O and at low impurity concentrations in CH_3OH and C_2H_5OH, both v_t and v_n increase with an increase in impurity concentration. Since an increase in v_n is associated with an enhanced rate of nucleation of monomolecular pits along the dislocation line, we may infer that in these cases impurity adsorption does not take place at the surface. The reason why surface adsorption is not favoured during dissolution at dislocation sites in CH_3OH and C_2H_5OH is the relatively higher heats of adsorption involved. Thus we conclude that during the selective etching of the {100} faces of NaCl crystals, the dependence of v_t and v_n on impurity concentration is, in general, associated with the adsorption of inhibiting species at both ledge and kink sites. However, the nature of the inhibiting species present in solution at different additive concentrations determines the absolute value of v_t and v_n.

In many cases etch rates markedly decrease and etch-pit formation is suppressed at very high impurity concentrations. This observation is likely to be connected with a decrease in crystal solubility in the presence of high concentration of an additive.

Most of the data reported in the literature [4, 12, 15] on the dependence of etch rates on additive concentration can be explained along the above lines. However, in order to interpret an increase in v_p, v_t and v_n of NaCl in CH_3COOH with increasing $FeCl_3$ concentration [15], it is necessary to assume that the crystal solubility is increased in the presence of this impurity.

4.1.3. Three-dimensional versus localized adsorption

The inhibiting action of impurities in changing the growth habit of crystals is believed to be due to three possibilities: (1) to the existence of epitaxial relationships with the three-dimensional structures of the habit-modifying substance or of compounds which it forms with the crystal substance and with the solvent medium [20, 35, 37–39], or (2) to changes in the thermodynamic and kinetic terms [40, 41], or (3) to change in crystal solubility [41]. Factors 2 and 3 change the rate of different faces to different extents and hence modify the crystal habit. The results [29, 42] obtained on the dependence of linear growth rates on impurity concentration show that kinetic effects are responsible for habit changes and that the energy of adsorption is several kcal mol^{-1} (1 cal = 4.18 J). According to Bliznakov [37, 43], who showed that surface coverage, θ, is related to growth rates by Equation 6, kinks are the active sites for impurity adsorption.

The idea of the formation of epitaxial layer has also been suggested to apply during the dissolution of alkali halides in solvents containing impurities [5]. Since the first work on LiF [1] however, it has repeatedly been suggested [3, 4, 6, 8, 12] that the inhibition of dissolution is caused at kink sites by the impurity cations. The low surface coverage of about 1% by the impurity species, noted in the present work, also excludes the possibility of the formation of a three-dimensional epitaxial layer on the dissolving surface. The dependence of dissolution rates on impurity concentration suggests that kinetic effects are responsible for the inhibition of dissolution. The values of the heats of adsorption indicate that the nature of adsorption during growth and dissolution is similar.

4.2. Formation and morphology of etch pits at dislocations

From the photographs of etch-pit patterns illustrated above and from Tables II and III, the following points may be noted.

1. In a particular solvent the lower the energy of adsorption of an impurity, the better is the contrast of etch pits.

2. For a particular impurity, the lower the

energy of adosrption in a solvent, the better is the contrast of etch pits. Thus the formation of contrasting etch pits is also associated with the ability of solvation of an impurity cation in a particular solvent.

From the observations presented here and from the literature [7, 12, 22] it follows that the concentration of an impurity required for the formation of etch pits of a particular orientation is less in a solvent in which the alkali halide is less soluble. It is also known [22] that the concentration of an impurity required for the formation of a particular chemical complex is less in a solvent in which the crystal is less soluble. This means that the morphology of etch pits is connected with the nature of chemical complexes present in solution. A similar conclusion was reached earlier [12]. However, in order to explain the change in the morphology of etch pits in the sequence $\langle 100\rangle \rightarrow \langle 110\rangle \rightarrow \langle 100\rangle$ observed with an increase in impurity concentration, it is necessary to postulate that adsorption of the inhibiting complexes present in solution takes place at ledges, isolated kinks and double kinks [22].

4.3. Undersaturation barrier for dislocation etch-pit formation

The two-dimensional theory of dislocation etch-pit formation, as developed by Cabrera and Levine [44] and Cabrera [45, 46] and by van der Hoek *et al.* [47], predicts the existence of an undersaturation barrier, given by

$$|\Delta\mu_c| \approx \frac{10\gamma^2\Omega\alpha}{Gb^2} \qquad (12)$$

for their nucleation. Here $\Delta\mu_c$ is defined by Equation 1, γ is the specific surface free energy, Ω the molecular volume, b the modulus of the Burgers vector of the dislocation, G the Shear modulus, and $\alpha = 2(1-\nu)$ and 2 for edge and screw dislocations respectively, and ν is the Poisson's ratio. In between $\Delta\mu = 0$ and $\Delta\mu = \delta\mu_c$, a stationary spiral dissolution process around a screw dislocation or a repeated two-dimensional process favoured by an edge dislocation may take place. For $\Delta\mu > \Delta\mu_c$, etch pits are formed at screw and edge dislocations by sponteneous nonstationary fast dissolution.

For the {100} plane of NaCl crystals, $G = 1.28 \times 10^4\,\mathrm{J\,cm^{-3}}$ [48], $b = 2^{1/2} \times 2.81 \times 10^{-8}\,\mathrm{cm}$, $\gamma = 1.3 \times 10^{-5}\,\mathrm{J\,cm^{-2}}$ in vacuum [49], and $\Omega = 1.025 \times 10^{-23}\,\mathrm{cm^3}$. At $T = 300\,\mathrm{K}$, for $\alpha = 2$ we obtain $\Delta\mu_c/kT = 0.41368$. Thus, using Equation 1, one obtains $(c/c_0)_{\mathrm{critical}} = 1.51$ or $\sigma_c = 0.51$.

In pure methanol the experimental σ_c is about 0.02, while in methanol containing 10^{-3} M $CdCl_2$ it is about 0.06. Although the theoretical value of σ_c is greater than the experimentally observed value, the experiments indicate that a critical undersaturation barrier does exist for dislocation etch-pit formation. The reason for the discrepancy between the experimental and theoretical values is probably associated with the lowering of γ in liquids [2, 50] and with the possible influence of diffusion processes [22].

4.4. Terracing of etch pits and surface roughening

Terracing of etch pits is a frequently encountered phenomenon and is usually explained in terms of either crystal structure [51] or beads of impurities perioidically segregated along the dislocation lines [52]. In the case of the {100} face of NaCl, terracing of pits was first observed in 1963 by Nadgornyi and Stepanov [13] during their etching experiments using acetic acid. These workers observed the formation of terraced etch pits at aged as well as fresh dislocations. The high density of dislocations in the NaCl crystals used in the present study makes it difficult to decide unambiguously whether the terraced pits are formed both at fresh and aged dislocations. However, the observation that all the etch pits produced on a surface by $CuCl_2 \cdot 2H_2O$ and $FeCl_3 \cdot 6H_2O$ (Figs. 4 and 6) are terraced indicates that they are formed at aged and fresh dislocations. The structure of NaCl lattice and the observation of terraced etch pits at aged and fresh dislocations suggest some other mechanism of terracing.

The development of rough surface by dissolution is also a usual observation [7, 8, 10, 12]. However, particular attention to this phenomenon was drawn in 1967 by Hari Babu and Bansigir [7, 8] during their experiments on the etching of the {100} surface of NaCl in ethanol containing $CdCl_2$ as poison. To date no satisfactory explanation of the phenomenon has been advanced.

Terracing of etch pits and surface roughening can be interpreted in terms of the formation of bunches of dissolution layers, i.e. by the kinematic theory of step motion. For this purpose we refer to Cabrera's curves of step flux against step density [22, 53, 54]. For systems in the absence of impurities a type I curve is obtained. According to this curve, positive bunching is possible at high fluxes of steps, i.e. at high dissolution rates, while

at lower fluxes the surface remains smooth. For etching systems containing impurities, there are type II and type III curves. A type II curve holds for low impurity concentrations and predicts negative bunching at very low fluxes whereas positive bunching is obtained at high fluxes. A type III curve is applicable for systems containing large concentrations of impurities [54]. In this case no bunching is possible at any flux and the surface remains smooth for all impurity concentrations. Below we apply these curves to interpret the terracing of etch pits and surface roughening, remembering that the step flux at dislocation sites is more than that at a surface free from defects.

It may be seen from the photographs of etch patterns that terraced etch pits are formed in pure CH_3OH and CH_3OH containing low concentrations of poorly effective impurities. In CH_3OH the rates are the highest. Therefore curves of types I and III may be applicable in this case. This means that here the surface should remain smooth while the pits may be terraced. In the case of highly effective impurity $CdCl_2$, curves of types II and III may be applied, which indicate that unterraced pits with a rough surface background are possible.

In the case of etching of the {100} faces of NaCl in CH_3OH containing $CuCl_2 \cdot 2H_2O$, some spiral etch pits with step heights of several tens nanometres were also observed (Fig. 6b). The fact that they are observed in 100% undersaturated methanol solution rules out the possibility that these spiral etch pits correspond to screw dislocations (cf Section 4.3). Further, the solubility of NaCl in H_2O, CH_3OH and C_2H_5OH is 0.36, 1.386×10^{-2} and 6.37×10^{-4} g ml^{-1}, respectively, at 25° C [55]. Using the relation between the fraction of the fluid space occupied by solute particles (i.e. the ratio of solute to the solid density), x_{seq}, and the surface entropy factor, α_J, given by [56]

$$\alpha_J = \xi(1 - x_{seq})^2(\Delta f_{sf} - \ln x_{seq}) \qquad (13)$$

with the surface anisotropy factor, $\xi = 0.5$, and the communal entropy, $\Delta f_{sf} = 1$, one obtains the surface entropy factor, α_J, to be 0.42, 2.45 and 4.06 for H_2O, CH_3OH and C_2H_5OH, respectively. Since for $\alpha_J > 4$, the surface is smooth and growth at low supersaturations is possible by screw dislocations [57, 58], the above values of α_J, by analogy with growth, imply that in H_2O and CH_3OH selective etching is possible only by two-dimensional dissolution process. The dependence of etch rates on undersaturation (Fig. 11) indeed indicates that for dissolution in CH_3OH and in CH_3OH containing $CdCl_2$ two-dimensional nucleation is the possible mechanism.

Thus we conclude that spiral etch pits may not always develop by spiral dissolution mechanism. An alternative mechanism, due to Lang [59], explains the formation of dissolution spirals having several monolayer thick steps in terms of the pinned nature of the spiral source and the deviation of the surface from its singularity.

4.5. Etch pits at fresh and aged dislocations

Except for $CdCl_2$ added to H_2O and CH_3OH, all other etching systems produce larger and deeper etch pits at the sites of aged dislocation than at fresh ones. In the case of $CdCl_2$ contained in C_2H_5OH even the morphology of etch pits at fresh and aged dislocations is different (Figs. 1b and c). For every etching system there is also a particular concentration of the impurity above which the pits at fresh and aged dislocations are indistinguishable.

Two mechanisms explain the formation of etch pits of different size at fresh and aged dislocations [1, 60]. The first mechanism postulates that the dislocation energy is reduced by segregated impurities. Since the rate of etch pit nucleation is directly connected with the dislocation energy [36, 44–47], according to this mechanism the etch rates at aged dislocations are reduced. The second mechanism assumes that, depending on the chemical nature (solubility) of an impurity segregated along the dislocation line, the etch rates are changed. Thus more soluble segregated impurities will lead to the formation of larger and deeper etch pits, while less soluble ones to smaller and shallower etch pits at aged dislocations. It is possible that in the same etching system both these mechanisms are operative, but, in general, one mechanism will dominate the other.

With reference to Tables II and III one may note that a difference between aged and fresh dislocation etch pits is exhibited by impurities involving the lowest heats of adsorption in slow solvents. Therefore it may be concluded that in the case of the etching of NaCl the chemical nature of an impurity segregated along the dislocation lines governs the distinction between etch pits at fresh and aged dislocations. The impurities dissolving from the dislocation lines may also be conceived to affect the morphology of etch pits and the values of etch rates v_t and v_n. When the

relative contribution by the dissolving segregated impurity to the total adsorption becomes much smaller, etch pits of almost the same size and morphology are formed at fresh and aged dislocations.

5. Conclusions

1. Langmuir and Temkin isotherms satisfactorily describe the data of the dependence of v_p on impurity concentration, c_i, in terms of surface coverage by the impurity. The value of the heat of adsorption is associated with the ability of solvation of an impurity cation in a particular solvent. The values of the heat of adsorption and the adsorption time indicate that adsorption is chemical in nature and that the inhibiting species remain immobile during crystal dissolution. The nature of the curves of v_t and v_n against c_i suggests that impurity adsorption takes place at ledge and kink sites.

2. The formation of dislocation etch pits is associated with the ability of solvation of an impurity cation in a particular solvent. The morphology of etch pits is likely to be connected with the nature of chemical complexes present in solution. The chemical nature of an impurity segregated along the dislocation line governs the difference between the morphology and size of etch pits at fresh and aged dislocations. The difference is due to the higher solubility of the impurities segregated along the dislocation lines.

3. In agreement with the two-dimensional nucleation theory involving the core or total energy of a dislocation, a critical undersaturation barrier exists for dislocation etch-pit formation on water-soluble crystals. Observation of the terracing of dislocation etch pits and the surface roughening can be interpreted by the kinematic theory of step motion.

Acknowledgements

The authors are grateful to Mrs B. Borecka for her assistance with the experimental data and to Dr J. Karniewicz for his keen interest in the work.

References

1. J. J. GILMAN, W. G. JOHNSTON and G. W. SEARS, *J. Appl. Phys.* **29** (1958) 747.
2. M. B. IVES and J. P. HIRTH, *J. Chem. Phys.* **33** (1960) 517.
3. S. MENDELSON, *J. Appl. Phys.* **32** (1961) 1579.
4. V. N. ROZHANSKII, E. V. PARVOVA, V. M. STEPANOVA and A. A. PREDVODITELEV, *Kristallografiya* **6** (1961) 704.
5. N. F. KOSTIN, S. V. LUBENETS and K. S. ALEKSANDROV, *ibid.* **6** (1961) 737.
6. A. A. URUSOVSKAYA, *ibid.* **8** (1963) 75.
7. V. HARI BABU and K. G. BANSIGIR, *J. Phys. Soc. Jpn.* **23** (1967) 860.
8. *Idem, J. Crystal Growth* **2** (1968) 9.
9. *Idem, J. Phys. Chem. Solids* **30** (1968) 1015.
10. *Idem, J. Appl. Phys.* **40** (1969) 827.
11. E. Yu. GUTMANAS and E. M. NADGORNYI, *Kristallografiya* **13** (1968) 114.
12. K. SANGWAL and A. A. URUSOVSKAYA, *J. Cryst. Growth* **41** (1977) 216.
13. E. M. NADGORNYI and A. V. STEPANOV, *Fiz. Tverd. Tela* **5** (1963) 998.
14. G. K. BARANOVA and E. M. NADGORNYI, *Kristallografiya* **17** (1972) 875.
15. *Idem, ibid.* **20** (1975) 446.
16. G. K. BARANOVA and E. M. NADGORNYI, *ibid.* **16** (1971) 596.
17. V. HARI BABU and K. G. BANSIGIR, *Ind. J. Pure Appl. Phys.* **8** (1970) 748.
18. B. SIMON, *J. Cryst. Growth* **52** (1981) 789.
19. M. A. VAN DAMME-VAN WEELE, in "Adsorption et Croissance Cristalline" (CNRS, Paris, 1965) p. 433.
20. H. E. BUCKLEY, "Crystal Growth" (Wiley, New York, 1951).
21. J. W. MULLIN, "Crystallization", 2nd edn. (Butterworths, London, 1972).
22. K. SANGWAL and A. A. URUSOVSKAYA, *Progr. Cryst. Growth Character.* in press.
23. S. N. ANDREEV and O. V. SAPOZHNIKOVA, *Zh. Neorg. Khimii* **10** (1965) 2538.
24. *Idem, ibid.* **13** (1968) 1548.
25. I. I. ANTIPOVA-KARATAEVA, Yu. A. ZOLOTOV and I. V. SERYAKOVA, *ibid.* **9** (1964) 1712.
26. R. VOSZKA, I. TARJAN, L. BERKES and J. KRAJSOVSZY, *Krist. Tech.* **1** (1966) 423.
27. K. SANGWAL and S. K. ARORA, *J. Mater. Sci.* **13** (1978) 1977.
28. K. SANGWAL, *ibid.* **17** (1982) 3598.
29. R. J. DAVEY and J. W. MULLIN, *J. Cryst. Growth* **26** (1974) 45.
30. Ya. GERASIMOV, V. DREVING, E. EREMIN, A. KISELEV, V. LEBEDEV, G. PANCHENKOV and A. SHLYGIN, "Physical Chemistry" Vol. 2 (Mir, Moscow, 1974).
31. J. OŚCIK, "Adsorption" (PWN-Polish Scientific Publishers, Warsaw, 1982).
32. A. A. CHERNOV, *Uspekhi Fizicheskikh Nauk* **73** (1961) 277.
33. *Idem*, in "Adsorption et Croissance Cristalline" (CNRS, Paris, 1965) p. 265.
34. I. GAJEWSKA, S. PIETRAS, J. RUDZIŃSKA and A. SCHELLENBERG (eds.), "Poradnik Fizykochemiczny" (Naukowo-Techniczne Press, Warsaw, 1974).
35. B. MUTAFTCHIEV, H. CHAJES and R. GINDT, in "Adsorption et Croissance Crystalline" (CNRS, Paris, 1965) p. 419.
36. W. SCHAARWÄCHTER, *Phys. Status Solidi* **12** (1965) 865.

37. R. KERN, in "Rost Kristallov" Vol. 8, Part 2 (Nauka, Moscow, 1968) p. 5.
38. P. HARTMAN, in "Adsorption et Croissance Cristalline" (CNRS, Paris, 1965) p. 477.
39. *Idem*, in "Crystal Growth: an Introduction", edited by P. Hartman (North-Holland, Amsterdam, 1973) p. 363.
40. F. C. FRANK, in "Adsorption et Croissance Cristalline" (CNRS, Paris, 1965) p. 513.
41. R. J. DAVEY, in "Industrial Crystallization 78" edited by E. J. de Jong and S. J. Jančić (North-Holland, Amsterdam, 1979) p. 169.
42. G. BLIZNAKOV and E. KIRKOVA, *Krist. Tech.* **4** (1969) 331; also see their other works cited therein.
43. G. BLIZNAKOV, *Fortschr. Mineral.* **36** (1958) 149.
44. N. CABRERA *and* M. M. LEVINE, *Phil. Mag.* **1** (1956) 450.
45. N. CABRERA, *J. Chim. Phys.* **53** (1956) 675.
46. *Idem*, in "The Surface Chemistry of Metals and Semiconductors", edited by H. C. Gatos (Wiley, New York, 1960) p. 71.
47. B. VAN DER HOEK, J. P. VAN DER EERDEN and P. BENNEMA, *J. Cryst. Growth* **56** (1982) 621.
48. K. H. HELLWEGE and A. M. HELLWEGE (eds) "Numerical Data and Functional Relationships in Science and Technology" Group III, Vol. 11 (Springer-Verlag, Berlin, Heidelberg, New York, 1979).
49. J. J. GILMAN, *J. Appl. Phys.* **31** (1960) 2208.
50. G. W. SEARS, *J. Chem. Phys.* **32** (1960) 1317.
51. J. W. FAUST, Jr, in "The Surface Chemistry of Metals and Semiconductors", edited by H. C. Gatos (Wiley, New York, 1960) p. 173.
52. J. J. GILMAN, *ibid.* pp. 172–3.
53. N. CABRERA and D. A. VERMILYEA, in "Growth and Perfection of Crystals", edited by R. H. Doremus, B. W. Roberts and D. Turnbull (Wiley, New York, 1958) p. 393.
54. J. BLOEM and L. J. GILING, in "Current Topics in Materials Science" Vol. 1 edited by E. Kaldis (North-Holland, Amsterdam, 1978) p. 147.
55. G. ZANIEWSKA, unpublished results (1983).
56. P. BENNEMA and J. P. VAN DER EERDEN, *J. Cryst. Growth* **42** (1977) 201.
57. G. H. GILMER and P. BENNEMA, *ibid.* **13/14** (1972) 148.
58. P. BENNEMA and G. H. GILMER, in "Crystal Growth: an Introduction" edited by P. Hartman North-Holland, Amsterdam, 1973) p. 263.
59. A. R. LANG, *J. Appl. Phys.* **28** (1957) 497.
60. W. G. JOHNSTON, in "Progress in Ceramic Science" Vol. 2, edited by J. E. Burke (Pergamon Press, Oxford, 1962) p. 1.

Received 7 April
and accepted 21 July 1983